baseline IRE-binding activity in tissues. However, the observation that IRE-binding activity can be recruited by oxidative disassembly of its Fe-S cluster means that in some pathological situations, including those in which inflammation results in release of reactive oxygen species, the vast reservoir of IRP1 in the aconitase form (Fig. 1C) may be converted to the IRE-binding form (*20*, *21*). This can lead to inappropriate repression of ferritin synthesis, increased TfR expression, and cellular iron toxicity. Increased iron content coupled with decreased ferritin has been observed in degenerating regions of the brain in Parkinson's disease (*28*). Thus, pathologic activation of IRP1 by reactive oxygen species may play an important role in some disease processes.

Our findings provide genetic evidence that in mammals, the tissue oxygen concentrations are a critical variable in regulating genes that are important in iron metabolism. Results obtained from tissue culture cells grown in room air may lead to conclusions that are not relevant to normal physiology. Iron- and oxygen-based chemistries affect many cellular processes, including mitochondrial function, DNA replication, and the response to hypoxia (*29*). Our work demonstrates that the IRP-regulatory system has evolved to tightly regulate iron metabolism at oxygen concentrations that exist in normal mammalian tissues. Even though the two IRPs are highly homologous (*1*), their activities are only partially redundant, and they occupy different regulatory niches. In normal physiology, tissue oxygen tension determines the contribution of each IRP to the regulation of iron homeostasis.

References and Notes

1. T. Rouault, R. Klausner, *Curr. Top. Cell. Regul.* **35**, 1 (1997).
2. B. D. Schneider, E. A. Leibold, *Curr. Opin. Clin. Nutr. Metab. Care* **3**, 267 (2000).
3. M. W. Hentze, M. U. Muckenthaler, N. C. Andrews, *Cell* **117**, 285 (2004).
4. H. Beinert, M. C. Kennedy, D. C. Stout, *Chem. Rev.* **96**, 2335 (1996).
5. B. Guo, J. D. Phillips, Y. Yu, E. A. Leibold, *J. Biol. Chem.* **270**, 21645 (1995).
6. K. Iwai *et al.*, *Proc. Natl. Acad. Sci. U.S.A.* **95**, 4924 (1998).
7. P. A. DeRusso *et al.*, *J. Biol. Chem.* **270**, 15451 (1995).
8. J. Wang, K. Pantopoulos, *Mol. Cell. Biol.* **22**, 4638 (2002).
9. E. G. Meyron-Holtz *et al.*, *EMBO J.* **23**, 386 (2004).
10. T. LaVaute *et al.*, *Nat. Genet.* **27**, 209 (2001).
11. Q. Chen *et al.*, *Proc. Natl. Acad. Sci. U.S.A.* **92**, 4337 (1995).
12. M. Erecinska, I. A. Silver, *Respir. Physiol.* **128**, 263 (2001).
13. P. O. Carlsson, F. Palm, A. Andersson, P. Liss, *Diabetes* **50**, 489 (2001).
14. L. Studer *et al.*, *J. Neurosci.* **20**, 7377 (2000).
15. E. S. Hanson, M. L. Rawlins, E. A. Leibold, *J. Biol. Chem.* **278**, 40337 (2003).
16. S. R. Smith *et al.*, *Ann. N. Y. Acad. Sci.* **1012**, 65 (2004).
17. S. R. Smith, T. A. Rouault, unpublished observations.
18. W. H. Tong, T. A. Rouault, *EMBO J.* **19**, 5692 (2000).
19. W. H. Tong *et al.*, *Proc. Natl. Acad. Sci. U.S.A.* **100**, 9762 (2003).
20. K. Pantopoulos *et al.*, *J. Biol. Chem.* **272**, 9802 (1997).
21. E. S. Hanson, E. A. Leibold, *Gene Expr.* **7**, 367 (1999).
22. C. Bouton, J. C. Drapier, *Sci. STKE* **2003**, pe17 (2003).
23. G. Cairo *et al.*, *Biochemistry* **41**, 7435 (2002).
24. K. Yamanaka *et al.*, *Nat. Cell Biol.* **5**, 336 (2003).
25. J. Wang *et al.*, *Mol. Cell. Biol.* **24**, 954 (2004).
26. L. S. Goessling, D. P. Mascotti, R. E. Thach, *J. Biol. Chem.* **273**, 12555 (1998).
27. E. Bourdon *et al.*, *Blood Cells Mol. Dis.* **31**, 247 (2003).
28. D. T. Dexter *et al.*, *Ann. Neurol.* **32** (suppl.), S94 (1992).
29. C. J. Schofield, P. J. Ratcliffe, *Nat. Rev. Mol. Cell Biol.* **5**, 343 (2004).
30. Materials and methods are available as supporting material on *Science* Online.

31. This work was supported by the intramural program of the National Institute of Child Health and Human Development and in part by the Lookout Foundation.

Supporting Online Material

www.sciencemag.org/cgi/content/full/306/5704/2087/DC1
Materials and Methods
Figs. S1 to S3
References

9 August 2004; accepted 22 October 2004
10.1126/science.1103786

Hepcidin Regulates Cellular Iron Efflux by Binding to Ferroportin and Inducing Its Internalization

Elizabeta Nemeth,[1] Marie S. Tuttle,[2] Julie Powelson,[2] Michael B. Vaughn,[2] Adriana Donovan,[3] Diane McVey Ward,[2] Tomas Ganz,[1]* Jerry Kaplan[2]*

Hepcidin is a peptide hormone secreted by the liver in response to iron loading and inflammation. Decreased hepcidin leads to tissue iron overload, whereas hepcidin overproduction leads to hypoferremia and the anemia of inflammation. Ferroportin is an iron exporter present on the surface of absorptive enterocytes, macrophages, hepatocytes, and placental cells. Here we report that hepcidin bound to ferroportin in tissue culture cells. After binding, ferroportin was internalized and degraded, leading to decreased export of cellular iron. The posttranslational regulation of ferroportin by hepcidin may thus complete a homeostatic loop: Iron regulates the secretion of hepcidin, which in turn controls the concentration of ferroportin on the cell surface.

The liver-produced hormone hepcidin controls plasma iron levels by regulating the absorption of dietary iron from the intestine, the release of recycled hemoglobin iron by macrophages, and the movement of stored iron from hepatocytes [for a review, see (*1*, *2*)]. During pregnancy, fetal hepcidin controls the transfer of maternal iron across the placenta to the fetus. In turn, hepcidin levels are homeostatically regulated by hepatic iron and by the need for erythropoiesis as sensed by liver oxygenation. Hepcidin is also induced during inflammation, in which hepcidin's effect on iron transport causes the characteristic decrease in blood iron (hypoferremia of inflammation). The hypoferremia is thought to increase host resistance to microbial infection but also leads to the anemia of inflammation (often referred to as the anemia of chronic disease).

Ferroportin (Fpn) is an iron exporter on the surface of absorptive intestinal enterocytes, macrophages, hepatocytes, and placental cells, all of which release iron into plasma (*3*–*5*). To determine whether hepcidin interacts with Fpn, we generated a stable cell line (HEK293-Fpn) expressing mouse Fpn with a C-terminal green fluorescent protein (GFP) under the control of the ecdysone-inducible promoter. In the absence of the inducer ponasterone, there was no detectable synthesis of Fpn-GFP. Within 24 hours of ponasterone addition, there was abundant GFP fluorescence outlining the surface of cells (fig. S1). To determine whether Fpn-GFP was functional, we examined the effect of ferroportin induction on cellular iron levels, as measured by the accumulation of ferritin, the cytosolic iron storage protein. Incubation of cells with ferric ammonium citrate (FAC) alone resulted in a large increase in ferritin levels. FAC loading with simultaneous induction of Fpn-GFP prevented ferritin accumulation (Fig. 1A). Similar results were obtained when diferric transferrin was used as an iron source and levels of IRP2, inversely regulated by cytosolic iron (*6*, *7*), were measured as an indicator of cellular iron levels (fig. S2). Induction of Fpn-GFP resulted in an increase of IRP2 levels when compared to uninduced cells, indicating that cytosolic iron levels decreased after the induction of Fpn-GFP. To show that reduced cytosolic iron levels re-

[1]Department of Medicine, David Geffen School of Medicine, University of California, Los Angeles, CA, USA. [2]Department of Pathology, School of Medicine, University of Utah, Salt Lake City, UT, USA. [3]Department of Hematology, Children's Hospital, Boston, MA, USA.

*To whom correspondence should be addressed. E-mail: TGanz@mednet.ucla.edu (T.G.); jerry.kaplan@path.utah.edu (J.K.)

sulted from Fpn-induced iron export rather than inhibition of iron uptake, cells were first incubated with FAC and then induced to express Fpn-GFP in the continued presence of FAC. Even with high levels of FAC in the medium, induction of Fpn resulted in a decrease in ferritin levels (Fig. 1B).

The addition of hepcidin to Fpn-GFP–expressing cells markedly changed the distribution of Fpn-GFP from the cell surface to punctate intracellular vesicles (Fig. 2A). Internalization of Fpn-GFP by hepcidin was observed even in the face of continued synthesis of Fpn-GFP. In the presence of the protein synthesis inhibitor cycloheximide, Fpn-GFP remained on the cell surface (fig. S3A), and only the addition of hepcidin caused the loss of surface Fpn-GFP and the appearance of Fpn-GFP in intracellular vesicles (fig. S3B). When hepcidin was removed from the medium, there was no recovery of cell surface fluorescence in the absence of proteins synthesis. Thus, once Fpn-GFP is internalized by hepcidin, it does not recycle to the cell surface.

Concentrations of hepcidin as low as 0.1 μM (0.3 μg/ml) induced Fpn internalization within 1 hour, whereas concentrations 10 times lower resulted in Fpn internalization over a 3-hour time course. These values are consistent with estimates of plasma hepcidin concentration based on urinary hepcidin excretion in either iron-loaded or infected individuals (*8*, *9*). Chemically synthesized hepcidin was as efficient in inducing Fpn-GFP internalization as was hepcidin purified from urine. Because hepcidin is a small cationic peptide, we considered the possibility that hepcidin-induced internalization of Fpn-GFP was nonspecific, because cationic peptides and proteins are known to induce endocytosis (*10*). Protegrin is a cationic antimicrobial peptide from pig neutrophils that is structurally similar to hepcidin (18 amino acids, cationic, beta-sheet, but only two disulfides) (*11*). The addition of protegrin to cells had little effect on the distribution of Fpn-GFP (fig. S4). Chemically synthesized truncated hepcidin lacking the five N-terminal residues (hep20) but retaining hepcidin conformation and most of the cationic residues (*12*) also had no effect on Fpn distribution or protein levels. Thus, hepcidin-induced Fpn-GFP internalization was specific for bioactive hepcidin (hep25).

Hepcidin had no effect on the distribution of another membrane receptor, epidermal growth factor receptor (EGFR) (Fig. 2B). Because EGFR can be better visualized in HeLa cells than in HEK293-Fpn cells, HeLa cells were transiently transfected with a plasmid expressing Fpn-GFP under the control of the cytomegalovirus (CMV) promoter. The addition of EGF, which induced the internalization of EGFR, had no effect on the distribution of Fpn-GFP, whereas the addition of hepcidin resulted in the internalization of Fpn-GFP but not EGFR.

Hepcidin induced not only internalization but also degradation of Fpn-GFP. In HeLa cells transfected with a plasmid containing a CMV-regulated Fpn-GFP, internalized Fpn-GFP colocalized with Lamp-1, a late endosomal/lysosomal marker (fig. S5). The addition of hepcidin to HEK293-Fpn cells for 4 hours caused the loss of Fpn-GFP (Fig. 3, A and B, and fig. S6). Chloroquine, an alkalinizing agent that inhibits lysosomal protease activity, prevented the hepcidin-induced loss of Fpn-GFP and increased Fpn-GFP fluorescence in intracellular vesicles, many of which colocalized with the lysosomal marker Lamp-1. Hep20 did not induce degradation of Fpn-GFP (fig. S6). These results demonstrate that Fpn-GFP internalized by hep25 is degraded in lysosomes.

We next examined whether hepcidin-mediated Fpn-GFP internalization affected iron transport. In the absence of hepcidin, induction of Fpn-GFP in cells exposed to FAC prevented the accumulation of ferritin, but the addition of increasing concentrations of hepcidin progressively increased cellular ferritin levels (Fig. 3C). Protegrin did not affect ferritin levels. Similarly, when cells were loaded with Tf(^{59}Fe)$_2$ and cellular iron levels were measured by the accumulation of radioactivity, induction of Fpn-GFP led to decreased radioactivity, whereas the addition of hepcidin to cells expressing Fpn-GFP led to an increase in radioactivity (Fig. 3D).

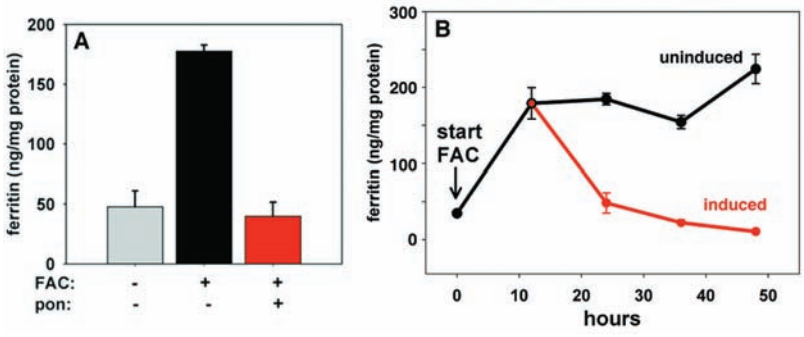

Fig. 1. Expression of a functional cell surface Fpn-GFP. (**A**) EcR293 cells were stably transfected with a plasmid containing an ecdysone-regulated Fpn-GFP construct. The resulting HEK293-Fpn cells were incubated with 10 μM FAC in the absence or presence of 10 μM ponasterone (pon) for 24 hours. Cells were harvested, and ferritin content was determined by enzyme-linked immunosorbent assay (ELISA). FAC addition resulted in increased ferritin, which was prevented by the simultaneous addition of ponasterone. (**B**) Cells were incubated with FAC for 12 hours. Ponasterone was then added to one set of cells (red line), and the cells were incubated in the continued presence of FAC for an additional 48 hours. Induction of Fpn-GFP decreased ferritin even in the presence of iron.

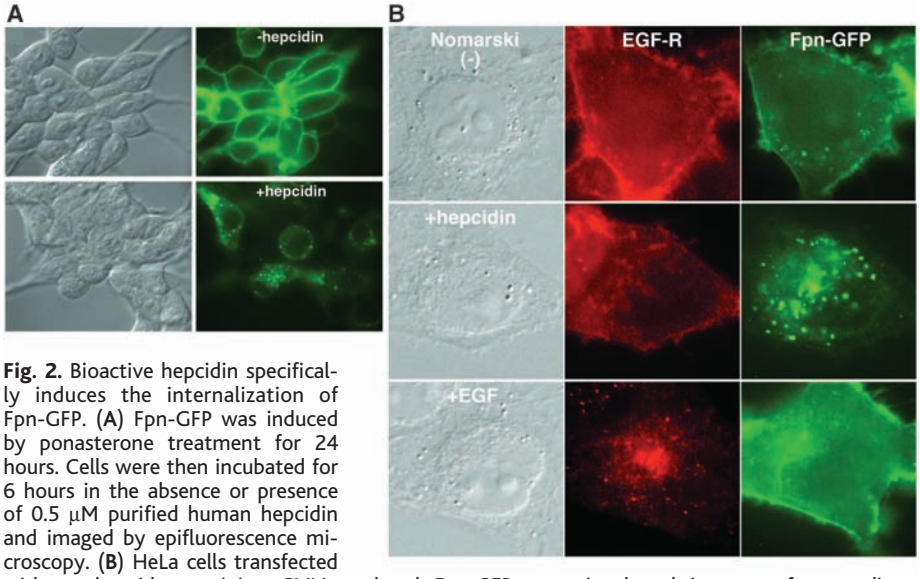

Fig. 2. Bioactive hepcidin specifically induces the internalization of Fpn-GFP. (**A**) Fpn-GFP was induced by ponasterone treatment for 24 hours. Cells were then incubated for 6 hours in the absence or presence of 0.5 μM purified human hepcidin and imaged by epifluorescence microscopy. (**B**) HeLa cells transfected with a plasmid containing CMV-regulated Fpn-GFP were incubated in serum-free medium overnight and then in the presence of cycloheximide (75 μg/ml) for 2 hours. In the continued presence of cycloheximide, cells were incubated, either with media alone (–), hepcidin (0.5 μM), or EGF (0.16 μM) for an additional 4.5 hours. The cells were processed for immunofluorescence and stained with a rabbit antibody to EGFR, followed by an Alexa 594 (red)–conjugated goat antibody to rabbit. Nomarski indicates the type of optics used to image the cells with a halogen lamp.

Hepcidin had no effect on uninduced cells. Thus, hepcidin prevents iron export by removing Fpn from the cell surface, which leads to cellular retention of iron.

We then determined whether hepcidin caused Fpn-GFP internalization by directly binding to Fpn. Human hepcidin contains two histidines that can be iodinated. The efficiency of hepcidin radioiodination, however, was low (specific activity 10^5 to 10^6 cpm/μg). We generated a modified hepcidin with a $Met^{21}\rightarrow Tyr^{21}$ substitution because tyrosine is present in this position in zebrafish hepcidin (GenBank accession number AAP80240). The modified hepcidin was as effective in inducing Fpn-GFP internalization as the unmodified peptide and allowed for a greatly increased efficiency of radioiodination (specific activity 5×10^7 cpm/μg). Cells expressing Fpn-GFP showed increased binding of ^{125}I-hepcidin relative to uninduced cells (Fig. 4A). Nonradioactive hepcidin competed with ^{125}I-hepcidin for binding to Fpn-GFP–expressing cells (with a median inhibitory concentration of about 700 nM), but protegrin or truncated hepcidin lacking the first five amino terminal residues (hep20) did not.

Cross-linking studies also indicated that hepcidin binds directly to Fpn. ^{125}I-hepcidin was cross-linked to cells uninduced or induced to express Fpn-GFP, and cellular lysates were either analyzed directly (Fig. 4B) or immunoprecipitated with an antibody to GFP (Fig. 4C). In both cases, ^{125}I-hepcidin was found in a band of the expected size for a complex of hepcidin–GFP-Fpn in ponasterone-induced but not -uninduced cells. No signal was detected when excess unlabeled hepcidin was added with iodinated hepcidin. The addition of protegrin did not prevent the binding of iodinated hepcidin. Thus, Fpn acts as the hepcidin receptor.

An inverse relation has been observed between hepcidin levels and Fpn protein or mRNA (*13*–*16*), but the mechanism underlying this relation is unclear. Most studies have focused on factors that affect Fpn mRNA levels. Fpn has a putative 5′ iron-responsive element (IRE), suggesting the possibility of regulation by the iron-binding proteins IRP1 and IRP2. Fpn protein levels, however, are inversely correlated with hepcidin mRNA even in mice with a mutation in the 5′ IRE of Fpn (*15*). Here we have found that Fpn levels can be regulated by direct interaction with hepcidin, resulting in the internalization and degradation of Fpn. The use of inducible or constitutive promoters that are iron-independent clearly separates the loss of Fpn from any effect on Fpn synthesis. Forced expression of Fpn in cultured cells results in a profound decrease in cytosolic iron (*3*), suggesting that the iron transport activity of Fpn is constitutive. Cellular iron export may be controlled by the concentration of Fpn at the cell surface, either through synthesis or, as shown here, through ligand-induced internalization and degradation.

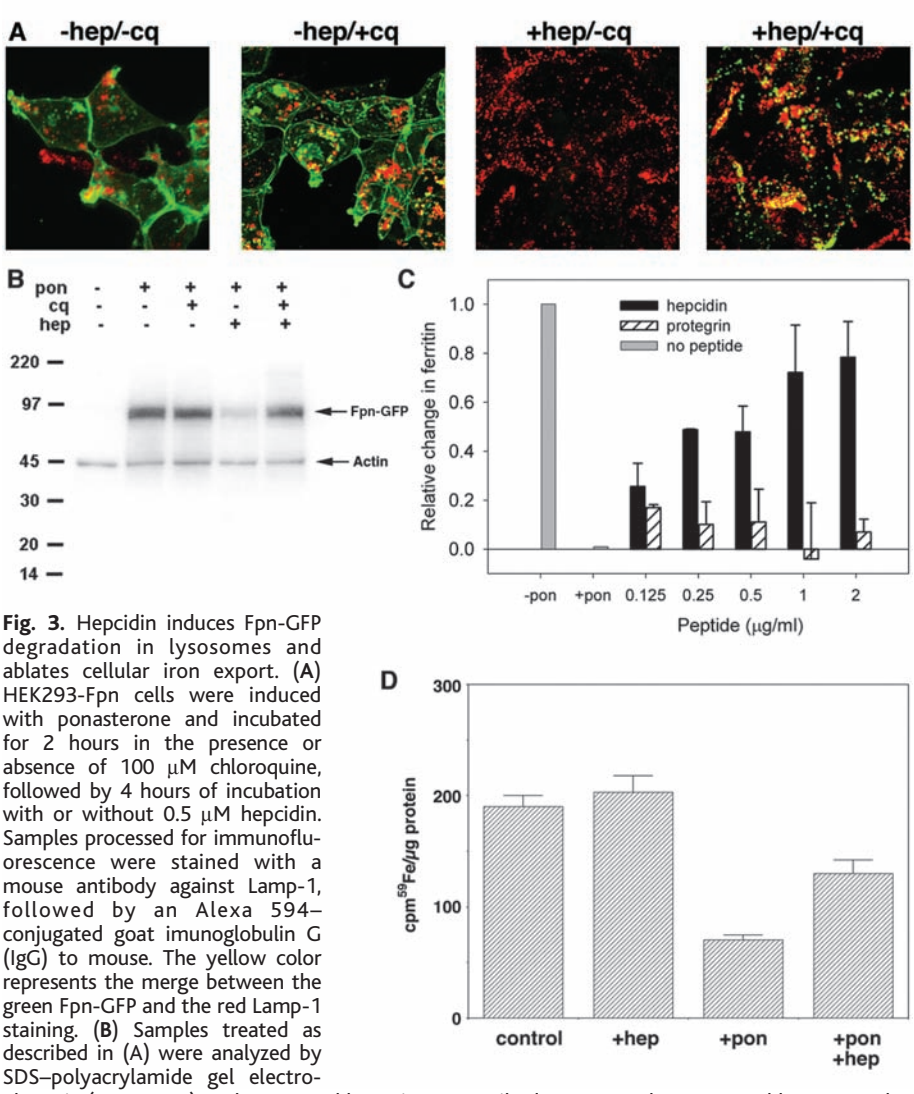

Fig. 3. Hepcidin induces Fpn-GFP degradation in lysosomes and ablates cellular iron export. (**A**) HEK293-Fpn cells were induced with ponasterone and incubated for 2 hours in the presence or absence of 100 μM chloroquine, followed by 4 hours of incubation with or without 0.5 μM hepcidin. Samples processed for immunofluorescence were stained with a mouse antibody against Lamp-1, followed by an Alexa 594–conjugated goat imunoglobulin G (IgG) to mouse. The yellow color represents the merge between the green Fpn-GFP and the red Lamp-1 staining. (**B**) Samples treated as described in (A) were analyzed by SDS–polyacrylamide gel electrophoresis (SDS-PAGE) and Western blot using an antibody to GFP. The Western blots were also probed with an antibody to actin to control for protein loading. (**C**) HEK293-Fpn cells were incubated for 24 hours with FAC. The cells were then induced with ponasterone in the presence or absence of the specified concentrations of hepcidin or protegrin for 24 hours. Cellular protein was extracted, and ferritin were concentrations determined by ELISA. The differences between hepcidin's and protegrin's effect on ferritin accumulation were statistically significant at each dose ($P < 0.01$ as determined by *t* test, except for the lowest dose $P < 0.05$). (**D**) Cells were incubated with 2.5×10^{-8} M Tf(^{59}Fe)$_2$ in the absence or presence of ponasterone or hepcidin (0.7 μM) for 12 hours. Cells were washed and cell-associated radioactivity was determined and normalized for total protein concentration.

Coupling the internalization of Fpn to hepcidin levels could generate a homeostatic loop regulating iron plasma levels and the tissue distribution of iron. Increased plasma iron, from macrophage recycling of aged red blood cells or from intestinal absorption of iron, stimulates hepatocytes by an as yet unknown mechanism to produce more hepcidin. Circulating hepcidin can bind to Fpn, cause its internalization, and trap iron in hepatocytes, macrophages, and absorptive enterocytes. The consequent rise in cytoplasmic iron could reduce iron uptake in these cells (*17*). Continued utilization of plasma iron, predominantly for hemoglobin synthesis by red cell precursors in the bone marrow, would rapidly deplete plasma iron, restoring the system to a steady state.

The hepcidin-ferroportin interaction may be central to the pathophysiology of hereditary hemochromatosis and the anemia of inflammation. Most types of hemochromatosis are characterized by hepcidin deficiency (*18*) or, less frequently, by autosomal dominant mutations of ferroportin (*18*). At the opposite end of the spectrum, in the anemia of inflammation, cytokine-stimulated hepcidin excess restricts the supply of iron for red cell production (*9*, *19*). Detailed analysis of hepcidin-Fpn interactions and Fpn internal-

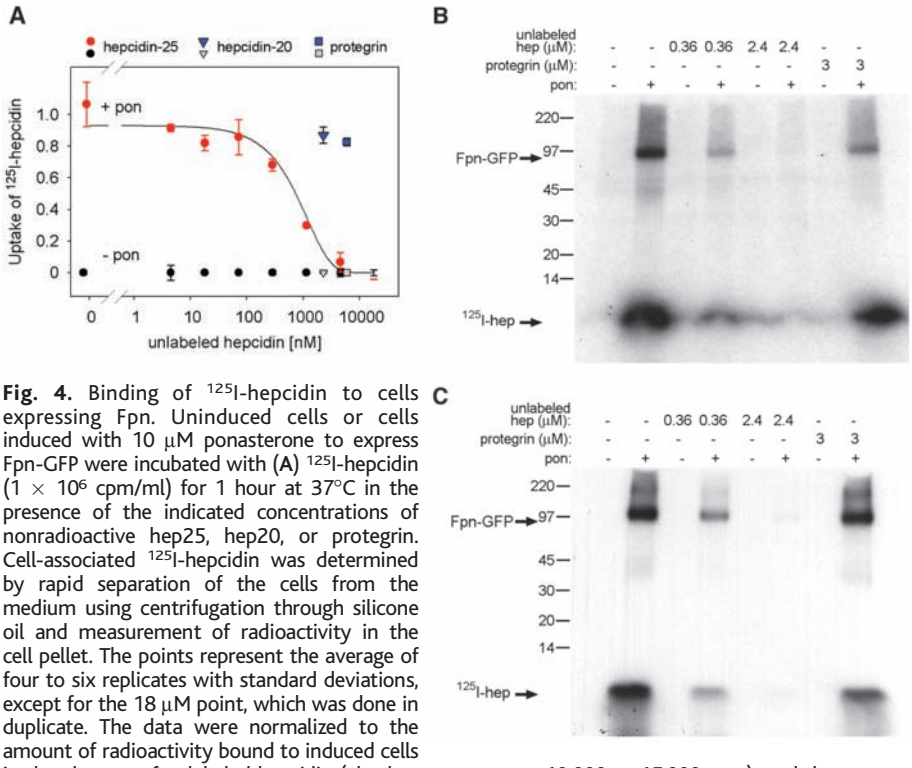

Fig. 4. Binding of ^{125}I-hepcidin to cells expressing Fpn. Uninduced cells or cells induced with 10 μM ponasterone to express Fpn-GFP were incubated with (**A**) ^{125}I-hepcidin (1×10^6 cpm/ml) for 1 hour at 37°C in the presence of the indicated concentrations of nonradioactive hep25, hep20, or protegrin. Cell-associated ^{125}I-hepcidin was determined by rapid separation of the cells from the medium using centrifugation through silicone oil and measurement of radioactivity in the cell pellet. The points represent the average of four to six replicates with standard deviations, except for the 18 μM point, which was done in duplicate. The data were normalized to the amount of radioactivity bound to induced cells in the absence of unlabeled hepcidin (absolute counts were 10,000 to 15,000 cpm), and the amount of radioactivity bound to uninduced cells (1000 to 3000 cpm) was subtracted as background for each point. (**B**) ^{125}I-hepcidin (1.5×10^6 cpm/ml) was added for 15 min at 37°C in the absence or presence of unlabeled hepcidin (hep) or protegrin and was cross-linked by the addition of 5 mM disuccinimidyl suberate (DSS). Cellular lysates (20 μg of total protein) were analyzed by SDS-PAGE and ^{125}I-hepcidin was visualized by autoradiography. Un–cross-linked ^{125}I-hepcidin that dissociated from Fpn during cell lysis is seen at the bottom of the gel. (**C**) Cellular lysates from (B) (400 μg of total protein) were immunoprecipitated with an antibody to GFP, separated by SDS-PAGE and ^{125}I-hepcidin visualized by autoradiography.

ization pathways should provide useful targets for the treatment of these iron disorders.

References and Notes

1. G. Nicholas *et al.*, *Blood Cells Mol. Dis.* **29**, 327 (2002).
2. T. Ganz, *Blood* **102**, 783 (2003).
3. S. Abboud, D. J. Haile, *J. Biol. Chem.* **275**, 19906 (2000).
4. A. T. McKie *et al.*, *Mol. Cell* **5**, 299 (2000).
5. A. Donovan *et al.*, *Nature* **403**, 776 (2000).
6. F. Samaniego, J. Chin, K. Iwai, T. A. Rouault, R. D. Klausner, *J. Biol. Chem.* **269**, 30904 (1994).
7. B. Guo, J. D. Phillips, Y. Yu, E. A. Leibold, *J. Biol. Chem.* **270**, 21645 (1995).
8. E. Nemeth *et al.*, *J. Clin. Invest.* **113**, 1271 (2004).
9. E. Nemeth *et al.*, *Blood* **101**, 2461 (2003).
10. H. J. Ryser, *Nature* **215**, 934 (1967).
11. A. Aumelas *et al.*, *Eur. J. Biochem.* **237**, 575 (1996).
12. H. N. Hunter, D. B. Fulton, T. Ganz, H. J. Vogel, *J. Biol. Chem.* **277**, 37597 (2002).
13. D. M. Frazer *et al.*, *Gastroenterology* **123**, 835 (2002).
14. K. Y. Yeh, M. Yeh, J. Glass, *Am. J. Physiol. Gastrointest. Liver Physiol.* **286**, G385 (2004).
15. H. Mok *et al.*, *Development* **131**, 1859 (2004).
16. F. Yang *et al.*, *J. Biol. Chem.* **277**, 39786 (2002).
17. M. Hentze *et al.*, *Cell* **117**, 285 (2004).
18. A. Pietrangelo, *N. Engl. J. Med.* **350**, 2383 (2004).
19. G. Nicholas *et al.*, *J. Clin. Invest.* **110**, 1037 (2002).
20. Molecular interaction data have been deposited in the Biomolecular Interaction Network Database (BIND) with accession code 181881. We thank J. P. Kushner and J. Hoidal for their critical reading of the manuscript. This work was supported by NIH grant DK065029 and the Will Rogers Fund to T.G. and by NIH grants HL26922 and DK30534 to J.K. M.S. was supported by NIH grant T35HL007744.

Supporting Online Material
www.sciencemag.org/cgi/content/full/1104742/DC1
Materials and Methods
Figs. S1 to S6
References

1 September 2004; accepted 8 October 2004
Published online 28 October 2004;
10.1126/science.1104742
Include this information when citing this paper.

Hemoxygenase-2 Is an Oxygen Sensor for a Calcium-Sensitive Potassium Channel

Sandile E. J. Williams,[1,5] Phillippa Wootton,[1] Helen S. Mason,[1,5] Jonathan Bould,[2] David E. Iles,[3] Daniela Riccardi,[5] Chris Peers,[4] Paul J. Kemp[1,5]*

Modulation of calcium-sensitive potassium (BK) channels by oxygen is important in several mammalian tissues, and in the carotid body it is crucial to respiratory control. However, the identity of the oxygen sensor remains unknown. We demonstrate that hemoxygenase-2 (HO-2) is part of the BK channel complex and enhances channel activity in normoxia. Knockdown of HO-2 expression reduced channel activity, and carbon monoxide, a product of HO-2 activity, rescued this loss of function. Inhibition of BK channels by hypoxia was dependent on HO-2 expression and was augmented by HO-2 stimulation. Furthermore, carotid body cells demonstrated HO-2–dependent hypoxic BK channel inhibition, which indicates that HO-2 is an oxygen sensor that controls channel activity during oxygen deprivation.

Large-conductance, Ca^{2+}-sensitive potassium (BK) channels are strongly implicated in the acute O_2 signaling cascade of a number of cellular systems. In carotid body chemoreceptors (*1*, *2*), low arterial pO_2 is detected by BK channels, and the resulting depolarizing signal is ultimately transduced into increased ventilation. BK channels in pulmonary arteriolar myocytes may contribute to both persistent prenatal (*3*) and acute postnatal hypoxic pulmonary vasoconstriction (*3*, *4*). Hypoxic inhibition of BK channels in perinatal adrenomedullary chromaffin cells is necessary for the catecholamine secretion crucial for preparing the newborn's lung to breathe air (*5*). Hypoxic depression of BK channel activity in neurons of the central nervous system (*6–8*) may also contribute to the excitotoxicity that results from increased neuronal excitability. As O_2 supply becomes compromised, BK channels are acutely and reversibly inhibited (*2*, *7–10*), resulting in cell depolarization. Subsequent voltage-gated Ca^{2+} influx induces hypoxia-dependent neurotransmitter release (*11*). In the carotid body, this ultimately results in increased ventilation. However, the molecular nature

[1]School of Biomedical Sciences, [2]School of Chemistry, [3]School of Biology, and [4]School of Medicine, University of Leeds, Leeds LS2 9JT, UK. [5]Cardiff School of Biosciences, Museum Avenue, Cardiff University, Cardiff, CF10 3US, UK.

*To whom correspondence should be addressed. E-mail: KempPJ@Cardiff.ac.uk